each trial. That model was rejected because it outperformed the dyads in experiment 2. This leaves open the possibility that the participants did communicate contrast and reliability, but used that information suboptimally, which seems unlikely, as we never observed any dyads explicitly communicating contrast and reliability separately. However, our data cannot definitively rule out this idea, and further research is needed to distinguish between optimal use of WCS versus suboptimal DSS.

The general consensus from extensive earlier work on collective decision-making is that groups rarely outperform their best members (*11*, *15*). Even in one of the rare cases in which consistent collaborative benefit was established, group performance failed to reach the bound predicted by the proposed ideal combination of individual decisions (*14*). That study employed the DSS model (see Eq. 4) to estimate the ideal, expected group sensitivity. As shown in experiments 1 and 2, however, the predictions of that model deviate significantly from empirical data if individuals' sensitivities differ markedly. In particular, experiment 2 demonstrated the detrimental side effect of collective decision-making based on Bayesian combination of confidence: Individuals with very different sensitivities are best advised to avoid collaboration and instead should rely entirely on the more sensitive individual. In fact, the WCS model and the results of experiment 2 (Fig. 3D) set a quantitative limit on the usefulness of cooperation that, to our knowledge, is not predicted by current economic and social theories of collective decision-making (*15*). An important next step for future research is to test the generality of this limit in other types of dyadic interactions.

Our findings have direct bearing on studies in social psychology that have discovered numerous situations in which groups fail to do better than their individuals. Many explanations for such "process loss" have been proposed, such as reduced effort in the presence of others [e.g., "social loafing" (*16*)], interpersonal competition (*11*), and groupthink (*17*). Our results raise the rather different possibility that, when the communicated evidence (perceived contrast) cannot be separated from its reliability (slope), such failures of collective decision-making may be the natural consequence of a perfectly reasonable strategy (for instance, WCS). Indeed, we know all too well about the catastrophic consequences of consulting "evidence" of unknown reliability on problems as diverse as the existence of weapons of mass destruction and the possibility of risk-free investments.

References and Notes

1. L. Bovens, S. Hartmann, *Bayesian Epistemology* (Oxford Univ. Press, Oxford, 2003).
2. S. Nitzan, J. Paroush, *Collective Decision Making: An Economic Outlook* (Cambridge Univ. Press, Cambridge, 1985).
3. D. Alais, D. Burr, *Curr. Biol.* **14**, 257 (2004).
4. M. O. Ernst, M. S. Banks, *Nature* **415**, 429 (2002).
5. K. P. Körding, D. M. Wolpert, *Nature* **427**, 244 (2004).
6. S. Deneve, P. E. Latham, A. Pouget, *Nat. Neurosci.* **4**, 826 (2001).
7. D. M. Green, J. A. Swets, *Signal Detection Theory and Psychophysics* (Wiley, New York, 1966).
8. W. J. Ma, J. M. Beck, P. E. Latham, A. Pouget, *Nat. Neurosci.* **9**, 1432 (2006).
9. For details of methods, models, and additional results, see the supporting material on *Science* Online.
10. G. W. Hill, *Psychol. Bull.* **91**, 517 (1982).
11. R. Hastie, T. Kameda, *Psychol. Rev.* **112**, 494 (2005).
12. P. R. Laughlin, A. L. Ellis, *J. Exp. Soc. Psychol.* **22**, 177 (1986).
13. In our model, this internal estimate of the probability of being correct is a function of the ratio of stimulus contrast in a given trial to its standard deviation. The standard deviation is found by fitting a cumulative Gaussian to the participant's psychometric function.
14. R. D. Sorkin, C. J. Hays, R. West, *Psychol. Rev.* **108**, 183 (2001).
15. N. L. Kerr, R. S. Tindale, *Annu. Rev. Psychol.* **55**, 623 (2004).
16. B. Latané, K. Williams, S. Harkins, *J. Pers. Soc. Psychol.* **37**, 822 (1979).
17. M. E. Turner, A. R. Pratkanis, *Organ. Behav. Hum. Decis. Process.* **73**, 105 (1998).

18. We thank D. Bang for generous help with data collection in experiments 2 and 4 and F. Scharnowski for his insightful comments in the early stages of the project. This work was supported by the European Union MindBridge project (B.B.), the Danish National Research Foundation and the Danish Research Council for Culture and Communication (A.R. and C.D.F.), the Gatsby Charitable Foundation (P.E.L.), and the Wellcome Trust (G.R.). Support from the MIND Lab UNIK initiative at Aarhus University was funded by the Danish Ministry of Science, Technology and Innovation.

Supporting Online Material

www.sciencemag.org/cgi/content/full/329/5995/1081/DC1
Materials and Methods
Figs. S1 and S2
References

8 December 2009; accepted 28 June 2010
10.1126/science.1185718

Phosphatidic Acid Is a pH Biosensor That Links Membrane Biogenesis to Metabolism

Barry P. Young,[1]* John J. H. Shin,[1]* Rick Orij,[2] Jesse T. Chao,[1] Shu Chen Li,[1] Xue Li Guan,[3,4] Anthony Khong,[5] Eric Jan,[5] Markus R. Wenk,[4,6,7] William A. Prinz,[8] Gertien J. Smits,[2] Christopher J. R. Loewen[1,9]†

Recognition of lipids by proteins is important for their targeting and activation in many signaling pathways, but the mechanisms that regulate such interactions are largely unknown. Here, we found that binding of proteins to the ubiquitous signaling lipid phosphatidic acid (PA) depended on intracellular pH and the protonation state of its phosphate headgroup. In yeast, a rapid decrease in intracellular pH in response to glucose starvation regulated binding of PA to a transcription factor, Opi1, that coordinately repressed phospholipid metabolic genes. This enabled coupling of membrane biogenesis to nutrient availability.

The hydrophobic portions of lipids can be sensed by hydrophobic protein domains that are often membrane inserted. Soluble protein domains recognize lipids by interacting predominately with their hydrophilic headgroups. Recruitment of proteins to membranes is dependent on the concentration of their target lipid in the bilayer. Membrane-associated transcription factors sense changes in the levels of key signaling lipids, enabling direct feedback regulation of lipid metabolism (*1*–*3*). In yeast, phospholipid metabolism is regulated by the transcriptional repressor Opi1, part of a lipid-sensor complex in the endoplasmic reticulum (ER) (fig. S1) (*3*). Opi1 is sequestered on the ER by binding both PA and the tail-anchored ER protein Scs2. Addition of inositol results in the rapid depletion of PA, release of Opi1 from the ER, and translocation of Opi1 to the nucleus (*3*). Nuclear Opi1 represses the Ino2/4 transcriptional activator complex, which binds a cis regulatory element, UAS_{INO}, found in many phospholipid metabolic genes (*4*).

Of the genes regulated by inositol and Opi1, *INO1* is the most highly regulated (*4*). *INO1* encodes the rate-limiting enzyme in inositol biosynthesis; thus, inositol auxotrophy is a sensitive measure of expression of the *INO1* gene and the status of the ER lipid sensor. We screened the

[1]Department of Cellular and Physiological Sciences, University of British Columbia, Vancouver, British Columbia, V6T 1Z3, Canada. [2]Department of Molecular Biology and Microbial Food Safety, University of Amsterdam, Amsterdam, 1018 WV, Netherlands. [3]Department of Biochemistry, Yong Loo Lin School of Medicine, National University of Singapore, Singapore 119077. [4]Department of Biochemistry, University of Geneva, Sciences II, 30 Quai Ernest Ansermet, CH-1211 Geneva, Switzerland. [5]Department of Biochemistry and Molecular Biology, University of British Columbia, Vancouver, British Columbia, V6T 1Z3, Canada. [6]Department of Biological Sciences National University of Singapore, Singapore 119077. [7]Swiss Tropical and Public Health Institute, University of Basel, Socinstrasse 57, P.O. Box 4002, Basel, Switzerland. [8]Laboratory of Cell Biochemistry and Biology, National Institute of Diabetes and Digestive and Kidney Diseases, National Institutes of Health, Bethesda, MD 20892, USA. [9]The Brain Research Centre, University of British Columbia, Vancouver, British Columbia, V6T 1Z3, Canada.

*These authors contributed equally to this work.
†To whom correspondence should be addressed. E-mail: christopher.loewen@ubc.ca

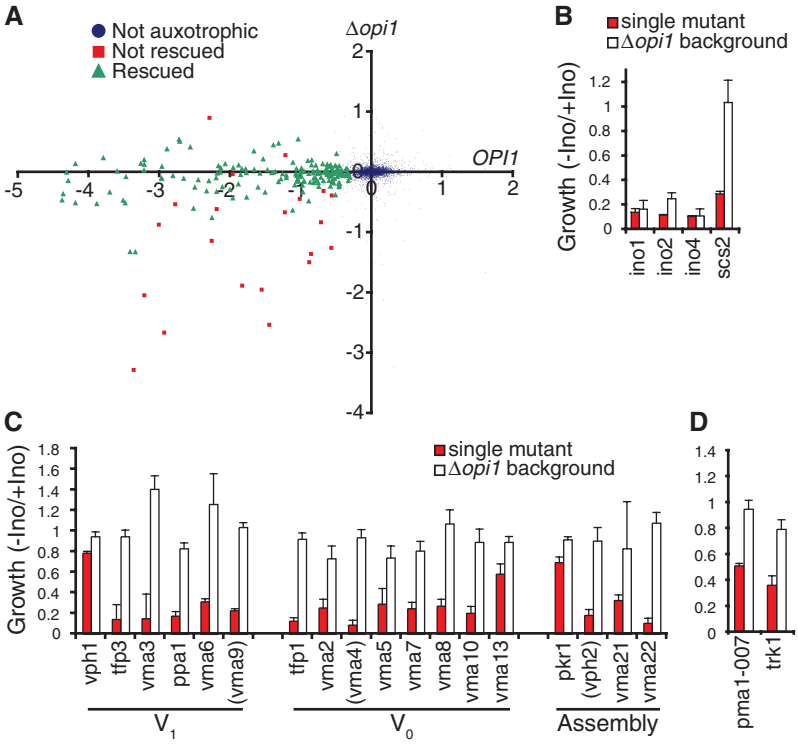

Fig. 1. Genome-wide screen for regulators of phospholipid metabolism. (**A**) Inositol auxotrophy of ~4800 deletion mutants and effect of deletion of *OPI1*. Plotted are $\log_2$ values of ratios of colony sizes for growth of mutants in the absence or presence of inositol (*5*). Single mutants are plotted on the *x* axis and double mutants with *Δopi1* on the *y* axis. (**B**) Inositol auxotrophy of known regulators of phospholipid metabolism and rescue by *Δopi1*. Plotted are ratios of colony sizes for growth of mutants in the absence (–Ino) or presence (+Ino) of inositol. (**C**) Inositol auxotrophy of V-ATPase deletion mutants. Mutants are grouped by V-ATPase domain (V_1, peripherally associated subunits; V_0, membrane-associated subunits) or factors required for V-ATPase assembly. Genes in parentheses indicate deletion of an overlapping dubious open reading frame and may not be true nulls. (**D**) Inositol auxotrophy of *pma1-007* and *Δtrk1* mutants. Error bars indicate SD.

haploid yeast deletion collection for sensitivity to growth in the absence of inositol (*5*). We identified 231 mutants with notable growth defects (fig. S2 and table S1). Most of these were rescued by deletion of Opi1 (Fig. 1A and table S2). The *Δino1*, *Δino2*, and *Δino4* mutants, which act downstream of the ER lipid-sensor, were not rescued (Fig. 1B). The *Δscs2* mutant was rescued as expected. Genes that govern intracellular pH (pH_i) were enriched in our data set (fig. S2 and table S3), including all 14 subunits of the vacuolar adenosine triphosphatase (V-ATPase) complex and the four factors in the ER responsible for its assembly (*6*) (Fig. 1C). The V-ATPase governs pH_i in part through regulation of Pma1 (*7*), a P-type H^+ ATPase of the plasma membrane (PM) that is the master regulator of pH_i (*8*). A hypomorphic allele of *PMA1* (*pma1-007*) that results in a 50% reduction in expression and activity of the Pma1 protein (*9*) was also an auxotroph (Fig. 1D). *TRK1*, a K^+ transporter of the PM that activates Pma1 (*7*), was also identified.

Because the *pma1-007* and *Δtrk1* mutants have an impaired capacity to pump protons out of the cell, they should be sensitive to acidification of the cytosol. To test this hypothesis, we subjected the strains to acid stress by growing them on medium buffered at low pH. Unlike in wild-type cells, pH_i in the *pma1-007* and *Δtrk1* mutants decreased with acidification of the medium (Fig. 2A). To determine whether cytosolic acidification causes derepression of Opi1, we measured transcription of Opi1-dependent genes by reporter assay (*3*) at pH 3, 4, and 5. We found almost complete repression in the *pma1-007* mutant at lowered pH, which was alleviated by deletion of *OPI1* (Fig. 2B and fig. S3). Wild-type cells showed a modest decrease in UAS_{INO} expression that was also dependent on *OPI1*. As expected, derepression of

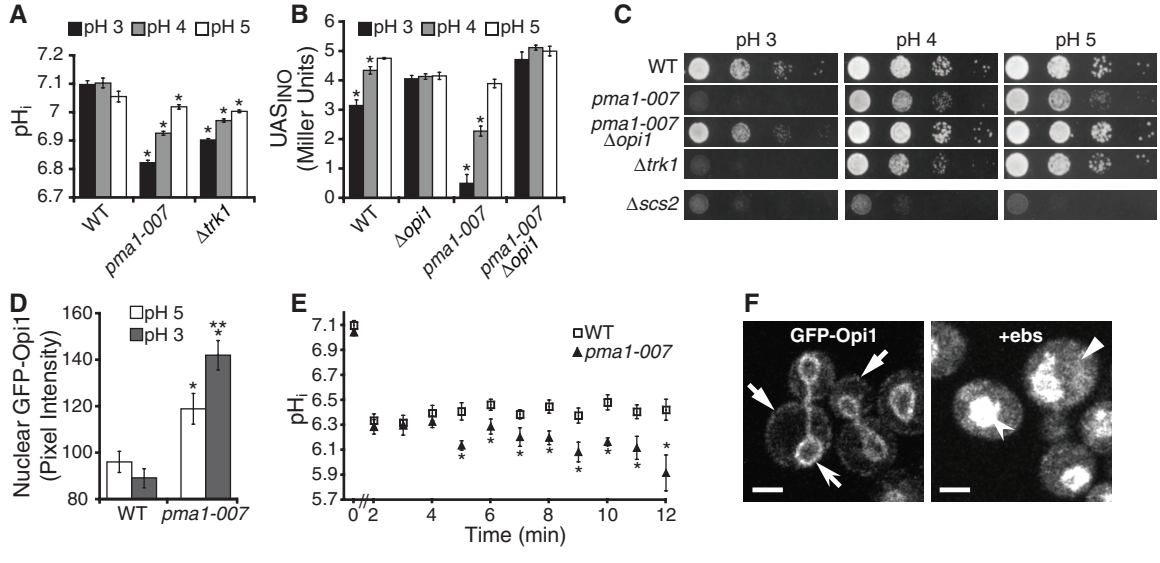

Fig. 2. pH regulates phospholipid metabolism. (**A**) pH_i of mutants grown in medium at pH 3, 4, and 5 compared to the wild type (WT) (*, versus WT at a given pH, $P < 0.001$). (**B**) UAS_{INO} reporter expression measured in different mutants grown at pH 3, 4, and 5 (*, versus pH 5, $P < 0.001$). (**C**) Growth of mutants in the absence of inositol at varying pH at 37°C. (**D**) Nuclear localization of GFP-Opi1 in cells grown at pH 3 and 5 quantified by confocal microscopy (*, versus WT at a given pH, $P < 0.005$; **, versus *pma1-007* at pH 5, $P < 0.01$). (**E**) Effect on pH_i after addition of 100 μM ebselen to WT and *pma1-007* cells grown in medium at pH 5 (*, versus WT at a given time point, $P < 0.05$). (**F**) Effect on the localization of GFP-Opi1 5 min after addition of 100 μM ebselen (+ebs). Arrows indicate ER localizations (straight, cortical; jagged, nuclear envelope); arrowheads indicate cytoplasmic (straight) and nuclear (jagged) localizations. Error bars indicate SEM in (A), (D), and (E) and SD (B). Scale bars, 2 μm.

Opi1 resulted in inositol auxotrophy of *pma1-007* and Δ*trk1* cells at low pH (Fig. 2C and fig. S4). This was in contrast to the Δ*scs2* mutant, which remained an inositol auxotroph at all pH values. Deletion of *OPI1* in the *pma1-007* mutant rescued its inositol auxotrophy at each pH. Opi labeled with green fluorescent protein (GFP-Opi1) accumulated in the nucleus of *pma1-007* cells, particularly at lowered pH (Fig. 2D), consistent with the decrease in UAS_{INO} expression. The drug ebselen, found to inhibit Pma1 in vitro (*10*), caused an immediate drop in pH_i of both wild-type and *pma1-007* cells to ~6.3 (Fig. 2E). Whereas wild-type cells stabilized at pH_i ~ 6.4, pH_i of *pma1-007* cells continued to decrease, indicating that the mutant is more sensitive, likely as a result of reduced gene dosage (*10*, *11*). Within 5 min, ebselen caused GFP-Opi1 to translocate from the ER to the cytosol and nucleus (Fig. 2F). Thus, pH_i regulates the localization and function of Opi1 and is a signal regulating transcription of phospholipid metabolic genes.

We examined whether pH affected the binding of Opi1 to PA. A basic domain in Opi1, Q2, directly binds the predominant pool of yeast PA, located in the PM (*3*). Ebselen caused GFP-Q2 to delocalize from the PM (Fig. 3A). This was also true for Spo20 (Fig. 3B), the other verified PA-binding protein in yeast (*12*). PM delocalization with ebselen was not due to endocytosis (fig. S5A). To control pH_i precisely, we treated yeast with the proton ionophore carbonyl cyanide 3-chlorophenylhydrazone (CCCP) over a range of pH values (*13*) and quantified GFP-Q2 localization to the PM (*5*). GFP-Q2 delocalized as pH decreased from 7.2 to 6.4 (Fig. 3, C and D). In contrast, localization of a probe for phosphatidylserine in the PM, GFP-Lact-C2 (*14*), did not change (fig. S5B). Thus, the binding of proteins to PA in vivo is sensitive to pH_i.

GFP-Q2 was delocalized in a V-ATPase mutant, Δ*vma2*, that had an acidified cytosol (Fig. 3, E and F). GFP-Lact-C2 localization was unaffected in this mutant (fig. S5C). Consistent with

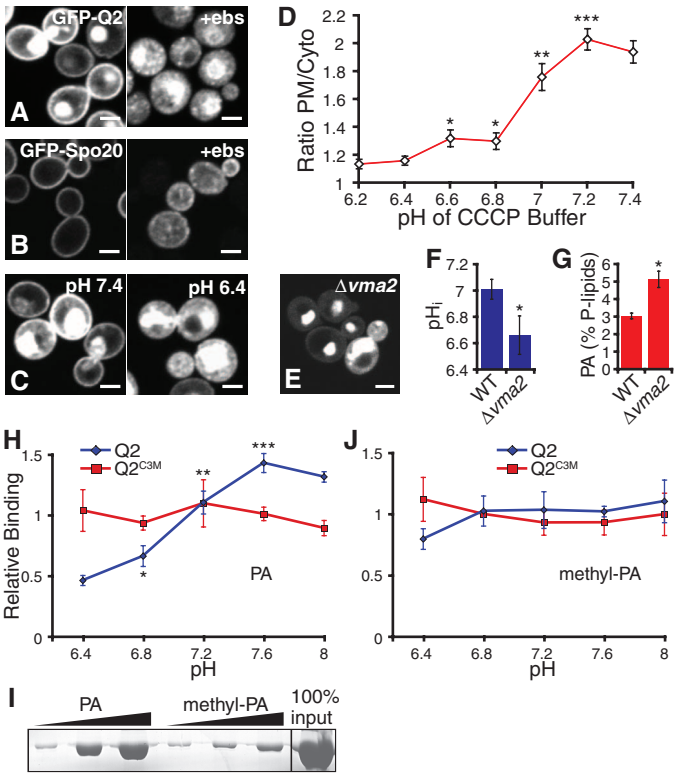

Fig. 3. pH governs the binding of Opi1 to PA through its protonation state. (**A**) Localization of GFP-Q2 after 5 min of ebselen treatment. (**B**) Localization of the PA-binding domain of Spo20 (GFP-Spo20$^{61\text{-}91}$) after 5 min of ebselen treatment. (**C**) Treatment of yeast expressing GFP-Q2 with CCCP buffered at the indicated pH. (**D**) Quantification of PM localization of GFP-Q2 with CCCP treatment (*, versus pH 6.4; **, versus pH 6.8; ***, versus pH 7; $P < 0.005$). (**E**) GFP-Q2 localization in Δ*vma2* cells. (**F**) pH_i measured in WT and Δ*vma2* cells grown in pH 5 medium (*$P < 0.0001$). (**G**) Total PA measured by mass spectrometry in WT and Δ*vma2* cells grown in pH 5 medium (*$P < 0.0001$). (**H**) Binding of Q2 and Q2^{C3M} to liposomes containing 10 mol % PA, 40 mol % phosphatidylethanolamine (PE) over a range of pH values (*, versus pH 6.4; **, versus pH 6.8; ***, versus pH 7.2; $P < 0.05$). (**I**) Binding of Q2 to liposomes (0, 100, 200 μM total lipid) containing 50 mol % PA or methyl-PA at pH 7.2. (**J**) Binding of Q2 and Q2^{C3M} to liposomes containing 20 mol % methyl-PA, 40 mol % PE over a range of pH values. Error bars indicate SD except in (D) (SEM). Scale bars, 2 μm.

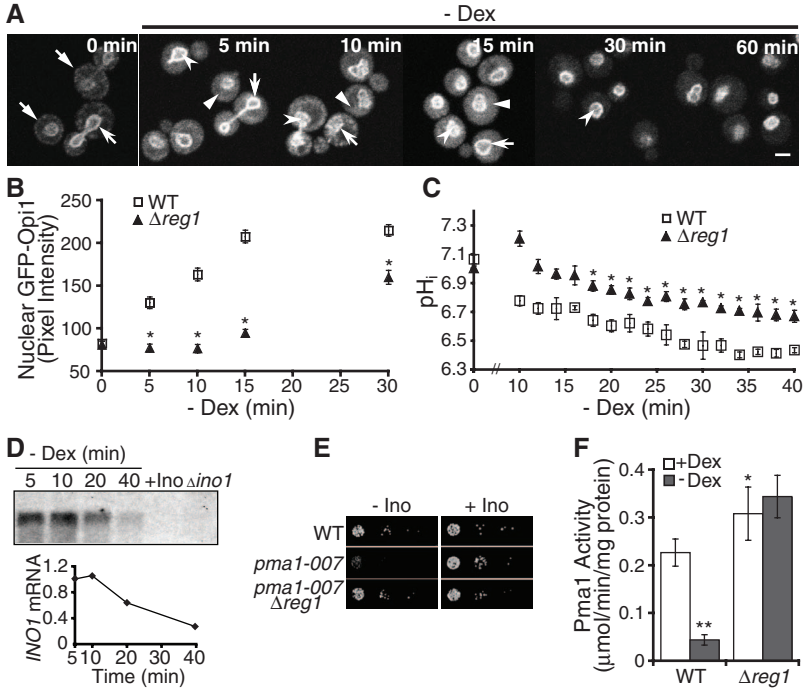

Fig. 4. Nutrient sensing and phospholipid metabolism are co-regulated by pH. (**A**) Localization of GFP-Opi1 in WT cells during glucose starvation. Time after removal from glucose (–Dex) is shown. Arrows and arrowheads as in Fig. 2. (**B**) Quantification of nuclear GFP-Opi1 after glucose starvation in WT and Δ*reg1* cells (*, versus WT at a given time point, $P < 0.0001$). (**C**) Change in pH_i measured in WT and Δ*reg1* cells during glucose starvation (*, versus $t = 0$ for Δ*reg1*, $P < 0.001$). (**D**) *INO1* mRNA levels during glucose starvation measured by Northern blot (+ Ino, cells grown in medium with inositol). (**E**) Growth of mutants at pH 4 in the presence or absence of inositol at 37°C. (**F**) Pma1 specific activity measured in WT and Δ*reg1* cells before and 20 min after glucose starvation (*, versus WT +Dex, $P < 0.05$; **, versus WT +Dex, $P < 0.005$). Scale bar, 2 μm.

an inability of Opi1 to bind PA in Δ*vma2* cells, GFP-Opi1 was translocated to the nucleus in this mutant, which also had decreased UAS_{INO} expression and was an inositol auxotroph (fig. S6). These phenotypes were not due to decreased PA levels, which were instead elevated ~70% in the mutant (Fig. 3G) (*5*). Thus, Opi1 failed to bind PA at lowered pH_i in this mutant.

Next, we bound recombinant Q2 to liposomes containing PA at varying pH (*5*). We found a near-linear increase in binding between pH 6.4 and 7.6 (Fig. 3H and fig. S7D). Three basic amino acids in Q2, $K_{136}K_{137}R_{138}$, are thought to participate in electrostatic interactions with the negatively charged headgroup of PA (*3*). Binding of the triple alanine substitution mutant ($Q2^{C3M}$) (*3*) to PA between pH 6.4 and 7.6 no longer depended on pH (Fig. 3H and fig. S7D). Thus, the direct interaction between Q2 and PA is sensitive to pH.

Unlike other phospholipids, the phosphate headgroup of PA is a monoester and has a second pK_a measured in model membranes to be between 6.6 and 7.9, depending on their phospholipid and protein composition (*15*, *16*). Changes in the ionization state of PA might thus be responsible for the observed pH-dependent binding of Opi1. We tested binding of Q2 to methyl-PA, which bears a methyl-group substitution on the phosphate and lacks the second pK_a (fig. S7A). Binding remained specific (fig. S7C), but was considerably weaker (Fig. 3I) and was pH independent (Fig. 3J and fig. S7D). Thus, Opi1 had higher affinity for deprotonated PA, consistent with the proposed electrostatic/hydrogen bond switch mechanism for the interaction of proteins with PA (*17*).

Because glucose-starved yeast exhibit a rapid drop in pH_i to ~ 6 (*7*) and our screen identified several major regulators of glucose signaling (fig. S8) (*5*), we hypothesized that glucose might be a physiological pH signal. Glucose starvation resulted in translocation of GFP-Opi1 from the ER to the nucleus (Fig. 4, A and B), which correlated with the drop in pH_i (Fig. 4C). *INO1* transcription was also repressed on a similar time scale (Fig. 4D). Translocation of GFP-Opi1 was not dependent on known modulators of PA levels (fig. S9) (*5*), suggesting that glucose acted independently of changes in the concentration of PA. Consistently, PA levels measured in ER microsomes isolated after 20 min of glucose starvation did not change significantly (fig. S10).

Reg1 is the glucose-signaling–specific regulatory subunit for Glc7, yeast's protein phosphatase type 1. Glc7 is implicated in repression of Pma1 (*18*), and Δ*reg1* yeast fail to repress *INO1* and overproduce inositol (*19*), suggesting that Reg1/Glc7 regulates pH_i through Pma1. Deletion of *REG1* rescued the inositol auxotrophy of the *pma1-007* mutant (Fig. 4E). Pma1 activity in the Δ*reg1* mutant was higher and failed to repress upon glucose starvation (Fig. 4F). Deletion of *REG1* attenuated the rapid drop in pH_i in glucose-starved cells (Fig. 4C). Thus, Reg1 repressed Pma1 in response to glucose starvation. GFP-Opi1 translocation was delayed in Δ*reg1* cells (Fig. 4B and fig. S9). In both wild-type and Δ*reg1* cells, translocation coincided with a drop in pH_i below 6.9, consistent with the reduced affinity of Opi1 for protonated PA.

Phosphatidic acid signaling can be dynamically regulated by changes in pH (fig. S11). This involves a change in the protonation state of the phosphate headgroup, making the lipid a pH biosensor. A pH-sensing role for lipids may not be limited to PA because phosphatidylinositol phosphates and ceramide-1-phosphate have pK_a values within the physiological range (*20*, *21*). Given the established roles for these lipids in signaling and the universality of pH regulation in biology, pH-dependent protein-lipid interactions may be important in a wide variety of systems.

References and Notes

1. J. L. Goldstein, R. A. DeBose-Boyd, M. S. Brown, *Cell* **124**, 35 (2006).
2. T. Hoppe *et al*., *Cell* **102**, 577 (2000).
3. C. J. Loewen *et al*., *Science* **304**, 1644 (2004).
4. G. M. Carman, S. A. Henry, *J. Biol. Chem.* **282**, 37293 (2007).
5. See supporting material on *Science* Online.
6. P. M. Kane, *Microbiol. Mol. Biol. Rev.* **70**, 177 (2006).
7. G. A. Martínez-Muñoz, P. M. Kane, *J. Biol. Chem.* **283**, 20309 (2008).
8. T. Ferreira, A. B. Mason, C. W. Slayman, *J. Biol. Chem.* **276**, 29613 (2001).
9. Z. Porat, N. Wender, O. Erez, C. Kahana, *Cell. Mol. Life Sci.* **62**, 3106 (2005).
10. G. Chan, D. Hardej, M. Santoro, C. Lau-Cam, B. Billack, *J. Biochem. Mol. Toxicol.* **21**, 252 (2007).
11. G. Giaever *et al*., *Nat. Genet.* **21**, 278 (1999).
12. H. Nakanishi, P. de los Santos, A. M. Neiman, *Mol. Biol. Cell* **15**, 1802 (2004).
13. R. Orij, J. Postmus, A. Ter Beek, S. Brul, G. J. Smits, *Microbiology* **155**, 268 (2009).
14. T. Yeung *et al*., *Science* **319**, 210 (2008).
15. A. Bhushan, M. G. McNamee, *Biophys. J.* **64**, 716 (1993).
16. E. E. Kooijman *et al*., *Biochemistry* **44**, 17007 (2005).
17. E. E. Kooijman *et al*., *J. Biol. Chem.* **282**, 11356 (2007).
18. T. Williams-Hart, X. Wu, K. Tatchell, *Genetics* **160**, 1423 (2002).
19. L. C. Hancock, R. P. Behta, J. M. Lopes, *Genetics* **173**, 621 (2006).
20. E. E. Kooijman, K. E. King, M. Gangoda, A. Gericke, *Biochemistry* **48**, 9360 (2009).
21. E. E. Kooijman *et al*., *Biophys. J.* **94**, 4320 (2008).

22. We are grateful to T. Levine for insight and critical reading of the manuscript; C. Boone for access to SGA technologies; M. Davies and L. Conibear for a preliminary inositol screen; and J. Church for discussions. This research was supported by grants from the National Sciences and Engineering Council of Canada (NSERC), the Canadian Institute of Health Research (CIHR), the Michael Smith Foundation for Health Research (MSFHR), the Canada Foundation for Innovation, and the British Columbia Knowledge Development Fund (C.J.R.L. and E.J.); the Intramural Research Program of the National Institute of Diabetes and Digestive and Kidney Diseases (W.A.P.); and the Singapore National Research Foundation under CRP Award 2007-04, the Biomedical Research Council of Singapore (R-183-000-211-305), the National Medical Research Council (R-183-000-224-213), and the SystemsX.ch RTD project LipidX (M.R.W.). J.J.H.S. is the recipient of a NSERC Alexander Graham Bell Canada Graduate Scholarship. C.J.R.L. is a CIHR New Investigator, a MSFHR Scholar, and a Tula Foundation Investigator.

Supporting Online Material

www.sciencemag.org/cgi/content/full/329/5995/1085/DC1
Materials and Methods
SOM Text
Figs. S1 to S11
Tables S1 to S3
References

16 April 2010; accepted 2 July 2010
10.1126/science.1191026